



# Tension Jamming for Deployable Structures

Daniel Hasegawa<sup>1</sup>, Buse Aktas<sup>2,1</sup> , *Member, IEEE*, Robert D. Howe<sup>1</sup>, *Fellow, IEEE*, 

**Abstract**—Deployable structures provide adaptability and versatility for applications such as temporary architectures, space structures, and biomedical devices. Jamming is a mechanical phenomenon with which dramatic changes in stiffness can be achieved by increasing the frictional and kinematic coupling between constituents in a structure by applying an external pressure. This study applies jamming, which has been primarily used in medium-scale soft robotics applications to large-scale deployable structures with components that are soft and compact during transport, but rigid upon deployment. It proposes a new jamming structure with a novel built-in actuation mechanism which enables high-performance at large scales: a composite beam made of rectangular segments along a cable which can be pre-tensioned and thus jammed. Two theoretical models are developed to provide insights into the mechanical behavior of the composite beams and predict their performance under loading. A scale model of a deployable bridge is built using the tension-based composite beams, and the bridge is deployed and assembled by air with a drone demonstrating the versatility and viability of the proposed approach for robotics applications.

**Index Terms**—Mechanism Design, Compliant Joints and Mechanisms, Soft Robot Materials and Design

## I. INTRODUCTION

Deployable robot structures are essential for applications like aerospace, medicine, and emergency infrastructure. These structures need to be collapsible, lightweight, and compact for easy transport, straightforward to deploy, and strong and large upon deployment for accomplishing tasks. There have been previous studies using a number of approaches, including rigid smaller modules that are assembled on site [1], linkage-based structures [2], inflatable structures [3], woven wire structures [4], pop-up structures [5], origami [6], and buckling-based structures [7]. These approaches have limitations for scaling up the structures while simultaneously ensuring ease of deployability and the ability to handle larger loads. This study presents a scaleable, programmable, and significant-load-bearing deployable structure using a novel type of jamming mechanism: composite beams with cables that apply a jamming force to the structure through active pre-tensioning. Jamming is a structural phenomenon in which an externally applied pressure to a collection of constituents increases the coupling between them, resulting in dramatic changes in stiffness of the overall structure [8], [9]. The jamming mechanism used in this study, which is built-in to

the composite structure, enables (1) larger and more scalable jamming forces than previously possible with primarily pneumatic jamming actuation methods, (2) structures that are easily compactable, transportable and deployable.

This paper begins by introducing jamming-based composite beams, which can easily transition from a low-stiffness collapsible compact state to a deployed high-stiffness state. Theoretical models characterizing the load-deflection behavior of the pre-tensioned composite beams are introduced, enabling an understanding of the effects of design parameters. The mechanical performance of the structure is experimentally determined and compared with the theoretical models. The benefits of using these beams in a deployable system are then demonstrated with the example of a drone-deployable bridge that is composed of three of the proposed beams assembled with connector elements.

## II. TENSION JAMMING-BASED COMPOSITE BEAMS

The beams are composed of rigid square prism segments that are threaded with a high-tensile strength cable through two holes. The aspect ratio of the cross-section of the beams are designed to take advantage of a small bending stiffness (second moment area) in one dimension when unjammed for easier rolling and compacting (Fig.1A) and a large bending stiffness in the orthogonal load-bearing dimension once jammed (Fig.1B). The cable is used to apply the jamming force. When tightened, the entire beam is straightened (if not already straightened) and the segments are forced together. The tension is applied with a ratcheting mechanism that is integrated into one end of the beam. Cable-based actuation methods have been used in some preliminary studies of jamming-based soft robots [10], [11]; however, they are at much smaller scales, and do not have a tensioning mechanism that is integrated to the structure (which enables structures that can remain jammed or unjammed without a tether). They also do not have the anisotropic bending stiffness which enables compactability in one direction and high bending stiffness in the other.

The jammed beams can be utilized as elementary modules to create more complex compound structures by incorporating pre-existing connection types used in joinery (e.g. lap joint, mortise and tenon joint) [12], robot-assisted construction [13], and modular robotics [14]. These compound structures can be used in a variety of robotic systems. For example, a truss-like structure could be used to form rigid links in a robot manipulator. The beams could also be used as masts in cable robots [15], and are particularly suited

<sup>1</sup> Paulson School of Engineering and Applied Sciences at Harvard University, Cambridge, MA, USA. dan62100dkh@gmail.com, howe@seas.harvard.edu <sup>2</sup> Institute of Robotics and Intelligent Systems, ETH Zurich, 8092 Zurich, Switzerland baktas@ethz.ch

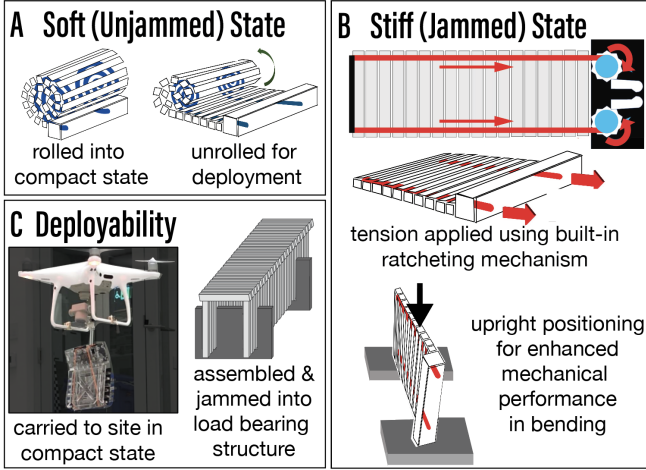


Fig. 1. Tension jamming-based composite beams, where a cable runs through the constituent rigid segments, along the entire length of the beam. A) In the unjammed state when the cable is loose, the beam can easily be rolled up and compacted. B) In the jammed state the cable is tightened with a built-in ratcheting mechanism, the tension from the cable creates compression on the segments, enabling the entire structure to act like one cohesive load-bearing beam, rather than individual segments. The structure's loading capabilities are enhanced when positioned upright. C) These beams can be used as modules to create load-bearing deployable structures.

for this application since they are strong in both bending and compression. Constructing components from these collapsible jamming-based beams enables robots and structures that can achieve a workspace and span much larger than the package from which it is initially deployed. And since the jamming mechanism is cable-driven, it can be actuated with a motor, enabling easy integration with existing automated robotic systems.

Additionally, the mechanical performance of the jammed structures can be predicted using theoretical models, enabling programmable design for desired performance criteria. The analytical models for the individual beams' performance can be based upon beam-bending equations, a well-understood field of continuum mechanics.

### III. MODELING AND CHARACTERIZATION OF MECHANICAL PERFORMANCE

To predict the mechanical performance of the jamming structures, we need to understand how the load is distributed throughout the composite beam and how it will deform when loaded. We take two theoretical approaches: (1) a pure bending model, in which the lower ends of the segments start spreading apart and (2) a shearing model, in which the segments slide with respect to each other. (Fig. 2)

#### A. Pure Bending Model

This model idealizes the beam's behavior as pure bending, assuming a constant radius of curvature, no frictional slip between the segments, and cables which are perfectly embedded in the beam. In this model, the internal stresses are calculated as a superposition of the stresses due to bending and the stress from the pre-tensioning.

According to Euler-Bernoulli beam theory, the flexural stiffness of a beam under bending is related to the effective elastic modulus of the composite beam  $E$ , the effective second moment of area  $I$ , and span length  $L$  by the following relationship  $\frac{\partial W}{\partial \delta} \propto \frac{EI}{L^3}$ , where  $W$  is the applied load and  $\delta$  is the resulting maximum deflection. A conventional beam with continuous material has a constant second moment of area resulting in constant stiffness. A beam with this construction, however, has three loading regimes in which the effective cross-section of the beam varies as a function of the stress distribution due to loading. The change in cross-section affects the second moment of area  $I$ , causing non-constant bending stiffness, and we have derived the equations to express the effective second moment of area in these three different regimes ( $I_1$ ,  $I_2$ , and  $I_3$ ), using the Young's Modulus of the segments for  $E$ .

In the first regime, the stress from the pre-tensioning dominates over that from bending, causing pure compression on the rigid segments, fully engaging the cross-section of the beam in the second moment of area. With the full beam engaged, the second moment of area is constant at its maximum value,  $I_1$ . This can be calculated using the parallel axis theorem

$$I_1 = n(2I_{cable} + 2Ad^2) + I_{segments} \quad (1)$$

where  $n$  is the ratio between the Young's moduli of the two materials:  $n = E_{cable}/E_{segments}$ ,  $A$  is the cross-sectional area of the cables, and  $d$  is the location of the cables with respect to the center of the beam  $d = H/2 - C$  (See Fig.2B for the dimensions on a diagram).

In the second regime, the stress distribution from bending begins to dominate, and the resulting tension at the bottom of the beam exceeds the compression caused by the prestress. The areas in which the rigid segments are no longer in compression do not contribute to the stiffness. This disengaged region increases in area as the load increases, growing upward from the bottom of the beam ( $x$  in Fig.2A), moving the effective neutral axis upward ( $y$  in Fig.2A), causing an effective second moment of area,  $I_2$ , that progressively and non-linearly decreases with applied load. In order to derive the expression for  $I_2$ , we solve a system of three equations: moment equilibrium, force equilibrium, and zero strain at neutral axis. The expression for  $I_2$  in terms of  $x$  and  $y$  is

$$I_2 = b(H-x) \left[ \frac{(H-x)^2}{12} + (\frac{x}{2} - y)^2 \right] + nA[(d+y)^2 + (d-y)^2] \quad (2)$$

where  $x$  and  $y$  depend on the applied weight  $W$  and the initial tension in the cable  $T_0$ , the solutions of which are

$$x = \frac{3LW - 4HT_0}{8T_0} \quad y = \frac{3LW - 4HT_0}{16T_0} \quad (3)$$

Per these expressions for  $x$  and  $y$ , region  $I_2$  begins when  $x, y > 0$  (as  $x = y = 0$  is when the full beam geometry is engaged and the neutral axis is in the middle of the beam). Accordingly, region  $I_2$  begins when the load  $W$  reaches the value  $\frac{4HT_0}{3L}$ . Additionally, we see that  $x$  and  $y$ 's rates of growth with respect to the loading  $W$  are inversely

proportional to  $T_0$ . Higher values of  $x$  and  $y$  reflect a smaller second moment of inertia, determined from Eq. 2.

The third regime occurs once the rigid segments have no section under compression, leaving the cables as the only contributors to the second moment of area. This would make the bending stiffness, reach a constant minimum,  $I_3$

$$I_3 = nA(H - C)^2 + nAC^2 \quad (4)$$

We can extend the bending model to not only predict the bending stiffness but also the failure load. The beam is expected to fail at the bottom cable (for most combinations of materials), where tensile stress from bending and the initial tensile stress from pre-tensioning combine. The load  $W$  at which the stress at the cable can be expressed as

$$\sigma_{bottomcable} = n \frac{WL(d + y)}{4I_i} + \frac{T_0}{A}. \quad (5)$$

When  $\sigma_{bottomcable}$  reaches the failure stress of the cable, the bridge is expected to fail. Using the above equations we can determine how the different geometric properties of the structure influence behavior, as well as how much pre-tensioning is appropriate for a given structure and loading condition. Specifically, while increased cable tension brings the stress in the bottom cable closer to its failure stress from before loading begins, it also results in a beam that stays in a stiffer state for higher loads. This direct trade-off can be managed by pre-tensioning the cable as much as possible given the cable's strength, the expected highest load on the structure, and the geometry of the components. Similar to conventional beams, this model predicts that increasing  $I$  increases stiffness and maximum loading. However, conventional geometries for doing so (I-beams, box beams, etc.) are not possible with a single sample of this composite, limiting the control of  $I$  to the aspect ratio of the rectangular

beam and  $I$ ,  $d$ ,  $A$ , and  $n$  for the cables. Specifically for  $I_1$ , the contribution from the segments grows with  $bH^3$ , while for the cables grows with  $nI_{cable}$  and  $nAd^2$ . From the failure stress relation, it can be determined that these correspond to maximum load growing with  $I_{cable}$ ,  $A$ ,  $d$ , and  $\frac{bH^3}{n}$ . The relative effect of cable versus segment geometry is accordingly highly dependent on their relative moduli,  $n$ .

### B. Shearing Model

This model concerns the shearing effects in the composite beam during loading. It has two regimes, separated by the point of slip, at which the shear force along the contact surfaces between the rigid segments is exactly equal to the friction force which depends on the initial tension in the cable  $T_0$ , and the coefficient of friction between the segments  $\mu_s$

$$W_{slip} = 4\mu_s T_0. \quad (6)$$

In the pre-slip regime, the rigid segments are held in position by static friction, resisting the internal shear forces caused by the applied load. This is expected to cause the beam to act as a contiguous solid piece, behaving exactly like the first regime in the previous model, with a second moment of area  $I_1$  which was described with Eq. 1.

After slip, the segments start sliding past each other. The overall shape of the beam resembles a letter "V", as shown in Fig. 2B. Cables conform to this shape, and the resulting vertical component of their tension would be the force acting against the applied load. Based on this sum of forces, the load-deflection regime is defined by the following equation

$$W(\theta) = 2EA(\sec\theta + \frac{T_0}{EA} - 1)\sin\theta \quad (7)$$

where  $\theta$  is the angle shown in Fig.2 (and the deflection,  $\delta$ , is directly trigonometrically dependent). The stiffness of this regime is based on this load-deflection behavior of the

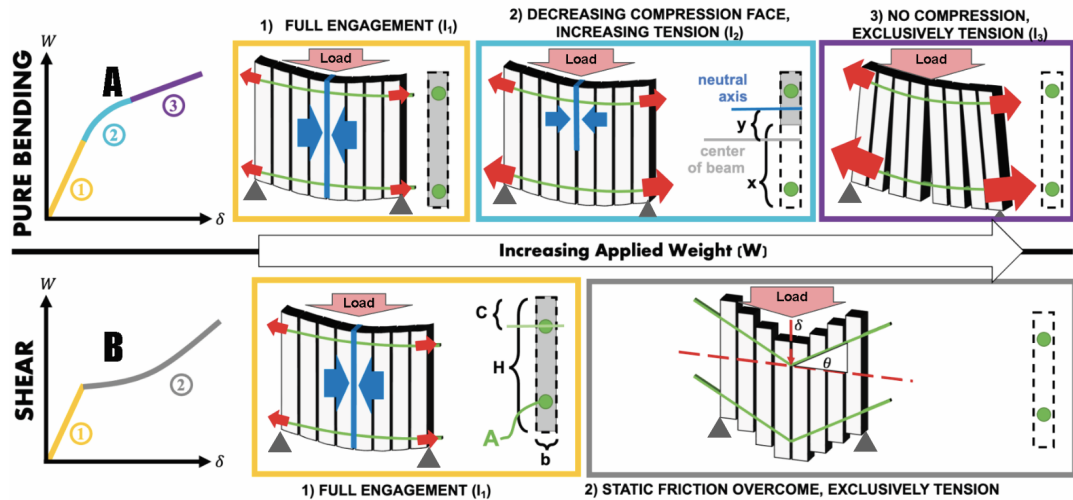


Fig. 2. Two theoretical models were used to predict the mechanical behavior of the beams in their jammed state. (A) The pure bending model calculates the changing effective second moment of area of the beam by considering the tension and compression along the beam caused by bending. The segments only contribute to the stiffness when under compression. (B) The shear model assumes a cohesive beam until the shear stress in the beam exceeds the friction between the segments. Afterward, the load is carried only with the cable.

cables, while the repeated settling and overcoming of the static friction will cause additional stick-slip behavior.

According to this model, the beam also fails due to tensile stress on the cables (for most relative cross-sectional areas and combinations of materials). The linear stress in them is defined by the following equation

$$\sigma_{cable}(\theta) = E(\sec(\theta) + \frac{T_0}{EA} - 1). \quad (8)$$

Two benefits of initial tensioning are determinable with this shearing model: (1) it increases the normal force between the segments, increasing the load required to overcome static friction, and (2) it improves stiffness in the second regime. Similarly to the pure-bending model, these come with the trade-off of a lower failure load, as initial tension in the cable brings it closer to its failure stress even before loading.

#### IV. IMPLEMENTATION EXAMPLE: DRONE-DEPLOYABLE BRIDGE

To demonstrate how the tension jamming-based composite beams can be used to create high-performance and versatile load-bearing deployable structures, we utilize them to build a novel rapidly deployable emergency bridge that can be delivered and assembled entirely through the air by rotorcrafts (drones or helicopters). Two parallel beams span the entire length of the bridge and are aligned on their vertical edge with the help of two anchors placed on either side of the span of the bridge. A tension jamming-based beam is also used to create a top mat to provide a loading surface. The deployment process of the multiple components take advantage of the tunability of the beams as shown in Fig.3. The two parallel beams are jammed before deployment to ensure the vertical placement and alignment without the beams collapsing, while the top mat is deployed in its unjammed state after one side is anchored. The top mat is jammed after it has been deployed.

Existing deployable bridges are primarily made of rigidly linked elements, include high-complexity components which increase cost and weight, and need to be delivered and deployed by large land vehicles [16]–[20]. Tension-jamming based beams propose a novel solution to this problem. By rolling into compact arrangements, the composite beams improve the rotorcraft delivery over significant possible distances to a deployment site. The jamming of the beams upon deployment enables a tunable-strength load-bearing bridge with a span much larger than the dimensions of the compacted beam.

##### A. Fabrication

A bridge with the span of 50 cm is built and tested for experimental validation. The drone used for deployment is the DJI Phantom 4 Pro V2 (DJI, Shenzhen, Guangdong, China), which has a maximum payload capacity of 800 grams. The segments of the bridge are constructed of acrylic using a laser cutter, with the dimensions 10x0.635x0.635 cm. The width is selected to match the depth so that each component is square in their vertical cross-sectional area.

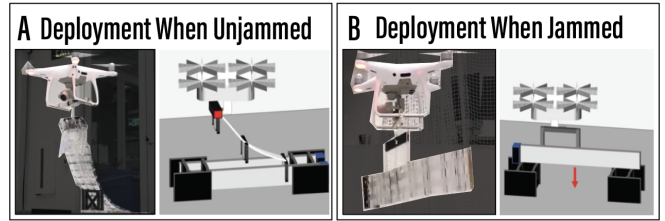


Fig. 3. Depending on assembly, the beams can be deployed either (A) in their unjammed state to be jammed after placement (top mat of bridge in implementation example) or (B) directly in their jammed state (main structural beams of bridge). Stills from the deployment of the bridge prototype are shown here, see supporting video for full deployment)

This enables a balance between promoting engagement between the component faces when jammed, and compliance for rolling up the pieces when unjammed.

##### B. Drone Deployment

The deployment of the bridge was successful, and a video showing the process is provided. The drone is flown manually by remote control by a pilot with no previous drone experience. The transit is done with ease, thanks to the compactness of the rolled-up beams. The deployment process is done with ease, thanks to the cables running through the segments, automatically aligning all components and the built-in tightening mechanism which stiffens the structure through tension jamming. The duration of the deployment process is between 10 and 20 minutes.

##### C. Mechanical Characterization

The bridge was tested in a mechanical testing machine (Instron 5566, Illinois Tool Works, Norwood, MA, USA), to experimentally characterize the force-deflection behavior and to validate the theoretical models for the composite beams. The tests were position-controlled, deflecting the structure a given deflection or in the final trial, until bridge failure. The results of these tests are shown in Fig. 4 including a direct comparison with the theoretical models developed.

An initial stiffness regime is observable in the load-deflection plot, as expected. The onset of the second loading regime is also a clear transition at around 80-100 Newtons. The process of rigid segments sliding past one another demonstrates a stick-slip behavior as expected after this transition point, and can be observed on the load-deflection plots. Sliding occurs when static friction is overcome, with the load temporarily decreasing as deflection increases. Additionally, the average load-deflection trajectory during this jagged behavior closely resembles the prediction of the shear-based model. While the post-slip effective stiffness matches the predictions from the shear model, the failure load seems to match the prediction from the pure bending model. Additionally, the structure failed by the snapping of the bottom cable, as predicted by our model. The bridge had an ultimate failure loading of around 380 N, and maximum stiffness of about 40,000 N/m.



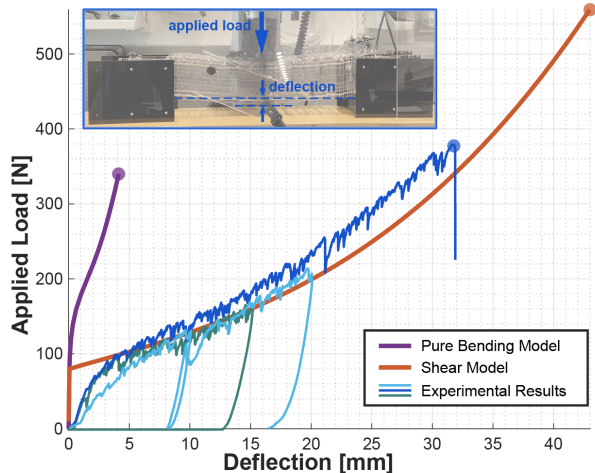


Fig. 4. Load-deflection behavior of the bridge prototype in fully jammed state. Three loading trials are shown (green, light blue, and dark blue curves) with maximum load increased for each trial until failure is reached on the third trial. Jagged curves are due to stick-slip sliding of the segments. Purple and orange curves are the pure bending and shear models, respectively. The points at the ends of the curves show failure loads. The post-slip stiffness matches the shear model, and the failure load matches the pure bending model.

## V. DISCUSSION

The novel tension jamming-based composite beam introduced, is designed with an aspect ratio such that it can be rolled up with ease with an effectively zero bending stiffness in one dimension when unjammed, and a high bending stiffness in the orthogonal direction once jammed. The tightening cable which runs through the entire beam allows it to be easily unrolled, deployed, and stiffened with a simple ratcheting mechanism. The beams can be designed to meet specific design specifications utilizing theoretical models. With their straightforward, versatile and modular design, they can easily be used as modules for the robotic construction of large-scale load-bearing jamming-based structures in a way that has not been achieved before. This was demonstrated in this paper through the drone-deployment of a scale model of a bridge based on these composite beams.

In addition to introducing an effective novel tunable composite beam design, this study developed two analytical models to predict the load-deflection and failure behavior, which were derived from first principles (force and moment balance, Hooke's law, static friction). The shearing-based model was accurate for the second loading regime of the bridge, where the static friction between the pieces was overcome and the tension in the cables acted against loading. The pure-bending model was valuable for providing a conservative estimate of the beam's failure load, in addition to providing far greater analytical understanding for beam-deflection in composite structures with changing effective cross-sections. Both models, particularly in the initial loading regime where the full geometry of the beam was expected to be engaged for maximum second moment of area and stiffness, significantly overestimated (factor of around 35) the

bending stiffness that was empirically observed in the first loading regime. Multiple causes for this can be considered. First, if the beams were leaning slightly off their vertical orientation, their corresponding second moment of area and therefore stiffness decreases considerably. Second, the shear deflection within the rigid segments could be non-negligible as the model assumes, resulting in a system in which the bending and shearing stiffness act together, again reducing the overall stiffness. The quantitative impact of both of these causes were modeled, yet neither accounted for the observed magnitude of difference. Further investigation into this discrepancy could consider if and how the size of the holes in the rigid segments could affect the string's engagement with the rest of the structure. Another consideration could be exactly how the beams rest in the anchor slots, which might be generating a boundary condition that cannot be approximated to a simple pin joint. Prior work on jamming has demonstrated how boundary conditions can influence mechanical performance, specifically resulting in the pre-slip stiffness values much lower than theoretically predicted [21]. While this paper only considered one pair of materials for cables and rigid components, further testing with other materials should be attempted to see the effect on stiffness, failure load, and how they match relatively to the analytical models. The limitations of the theoretical models could be further addressed by designing experiments to investigate the validity of the assumptions made regarding the mechanical interactions between the constituents of the beam. For example, strain gauges or load cells could be used to determine the change in tension in the top and bottom cables within the structural beams throughout loading. Pressure sensors between rigid segments could be placed to determine the change in the pressure distribution with loading. These empirical insights regarding inter-constituent interactions within the beam can also be supported by simulations that are based on finite element analysis and kinematics. Before full large-scale robotic structures are made, the models need to be improved and validated at various intermediate scales. Additionally, at larger scales the model would likely need to include the weight of the material of the beams, which were neglected in this study.

There have been some studies applying jamming to larger-scale structures, but none of them, to our knowledge, has the functionality and deployability achieved in this study. They all require complex construction processes with large-scale robotic arms and need to be deployed by land [22], [23]. We have shown, through the drone-based deployment process of a bridge, that our tension-jamming-based approach results in a deployment process that is much more straightforward to automate. The process has much fewer steps in the assembly sequence, reducing the sources of error. Simple specialized segments can be integrated into the beam to assist with the deployment and assembly process, reducing the need for precision on the robot end. The tension jamming-based beams can also be integrated with other existing deployable

robotic structure solutions, to achieve higher-performance deployability. For example, there have been studies utilizing drones to construct load-bearing structures which contain a large number of rigid modules that are assembled in a way resembling masonry [24]–[26]. By using our large span beams rather than individual small brick-like elements, we can create a much more efficient deployment process and also enable the construction of more complex structures. Another application area would be deployable space structures. Existing systems typically include a combination of rigid and soft elements, in which the rigid elements (e.g. booms, struts) are not collapsible [27]–[29]. Our beams would enable these rigid segments to become collapsible, making the overall space structure even more compact during delivery.

## VI. CONCLUSION

Tension jamming based composite beams for easily deployable, scalable, load-bearing robotic structures were introduced. The beams can easily transition between a rigid, structural, load bearing form, and a compact, transportable form. Two analytical models derived from first principles provide insights into the mechanical phenomena occurring within the beam under loading, enable predicting the failure load and load-deflection behavior and provide insights into how different design parameters influence performance. These beams were then utilized to create a drone-deployable bridge, demonstrating the ease of deployability of the beams as modules for larger scale structures. The mechanical performance of the resulting structure was characterized, experimentally validating the theoretical model.

## ACKNOWLEDGMENTS

The authors would like to thank Steve Cortesa, Linsey Moyer, Greg Freeburn, Sebastian Roubert Martinez, Andrew Chin, and Alan and Lise Hasegawa.

## REFERENCES

- [1] B. Salemi, M. Moll, and W.-M. Shen, "Superbot: A deployable, multi-functional, and modular self-reconfigurable robotic system," in *2006 IEEE/RSJ International Conference on Intelligent Robots and Systems*. IEEE, 2006, pp. 3636–3641.
- [2] X. Zhang, R. Nie, Y. Chen, and B. He, "Deployable structures: Structural design and static/dynamic analysis," *Journal of Elasticity*, vol. 146, no. 2, pp. 199–235, 2021.
- [3] P. Palmieri, M. Melchiorre, and S. Mauro, "Design of a lightweight and deployable soft robotic arm," *Robotics*, vol. 11, no. 5, p. 88, 2022.
- [4] M. Shahinpoor and B. Smith, "Deployable robotic woven wire structures and joints for space applications," in *NASA, Lyndon B. Johnson Space Center, Fourth Annual Workshop on Space Operations Applications and Research (SOAR 90)*, 1991.
- [5] E. E. Montano and E. A. Peraza Hernandez, "Kinematic design of deployable structures with low actuation requirements based on pop-up folding," in *International Design Engineering Technical Conferences and Computers and Information in Engineering Conference*, vol. 85444. American Society of Mechanical Engineers, 2021, p. V08AT08A031.
- [6] D. Rus and M. T. Tolley, "Design, fabrication and control of origami robots," *Nature Reviews Materials*, vol. 3, no. 6, pp. 101–112, 2018.
- [7] S. Mhatre, E. Boatti, D. Melancon, A. Zareei, M. Dupont, M. Bechthold, and K. Bertoldi, "Deployable structures based on buckling of curved beams upon a rotational input," *Advanced Functional Materials*, vol. 31, no. 35, p. 2101144, 2021.
- [8] Y. S. Narang, J. J. Vlassak, and R. D. Howe, "Mechanically versatile soft machines through laminar jamming," *Advanced Functional Materials*, vol. 28, no. 17, p. 1707136, 2018.
- [9] B. Aktaş, Y. S. Narang, N. Vasios, K. Bertoldi, and R. D. Howe, "A modeling framework for jamming structures," *Advanced Functional Materials*, vol. 31, no. 16, p. 2007554, 2021.
- [10] Y. Jiang, D. Chen, C. Liu, and J. Li, "Chain-like granular jamming: a novel stiffness-programmable mechanism for soft robotics," *Soft robotics*, vol. 6, no. 1, pp. 118–132, 2019.
- [11] P. M. Loschak, S. F. Burke, E. Zumbro, A. R. Forelli, and R. D. Howe, "A robotic system for actively stiffening flexible manipulators," in *2015 IEEE/RSJ International Conference on Intelligent Robots and Systems (IROS)*. IEEE, 2015, pp. 216–221.
- [12] S. E. van Nimwegen and P. Latteur, "A state-of-the-art review of carpentry connections: From traditional designs to emerging trends in wood-wood structural joints," *Journal of Building Engineering*, p. 107089, 2023.
- [13] R. B. Fleischman, B. V. Viscomi, and L.-w. Lu, *ATLSS Connections: Concept, Development and Experimental Investigation*. Lehigh University, ATLSS Engineering Research Center, 1991.
- [14] S. Chennareddy, A. Agrawal, A. Karuppiah *et al.*, "Modular self-reconfigurable robotic systems: a survey on hardware architectures," *Journal of Robotics*, vol. 2017, 2017.
- [15] S. Qian, B. Zi, W.-W. Shang, and Q.-S. Xu, "A review on cable-driven parallel robots," *Chinese Journal of Mechanical Engineering*, vol. 31, no. 1, pp. 1–11, 2018.
- [16] G. E. Fenci and N. G. Currie, "Deployable structures classification: A review," *International Journal of Space Structures*, vol. 32, no. 2, pp. 112–130, 2017.
- [17] L. Puig, A. Barton, and N. Rando, "A review on large deployable structures for astrophysics missions," *Acta astronautica*, vol. 67, no. 1–2, pp. 12–26, 2010.
- [18] W. M. Sokolowski and S. C. Tan, "Advanced self-deployable structures for space applications," *Journal of spacecraft and rockets*, vol. 44, no. 4, pp. 750–754, 2007.
- [19] I. Ario, M. Nakazawa, Y. Tanaka, I. Tanikura, and S. Ono, "Development of a prototype deployable bridge based on origami skill," *Automation in construction*, vol. 32, pp. 104–111, 2013.
- [20] B. R. Russell and A. P. Thrall, "Portable and rapidly deployable bridges: Historical perspective and recent technology developments," *Journal of Bridge Engineering*, vol. 18, no. 10, pp. 1074–1085, 2013.
- [21] B. Aktaş and R. D. Howe, "Flexure mechanisms with variable stiffness and damping using layer jamming," in *2019 IEEE/RSJ International Conference on Intelligent Robots and Systems (IROS)*. IEEE, 2019, pp. 7616–7621.
- [22] P. Aejmelaeus-Lindström, J. Willmann, S. Tibbits, F. Gramazio, and M. Kohler, "Jammed architectural structures: towards large-scale reversible construction," *Granular Matter*, vol. 18, no. 2, pp. 1–12, 2016.
- [23] G. Rusenova, F. K. Wittel, P. Aejmelaeus-Lindström, F. Gramazio, and M. Kohler, "Load-bearing capacity and deformation of jammed architectural structures," *3D Printing and Additive Manufacturing*, vol. 5, no. 4, pp. 257–267, 2018.
- [24] S. Goessens, C. Mueller, and P. Latteur, "Feasibility study for drone-based masonry construction of real-scale structures," *Automation in Construction*, vol. 94, pp. 458–480, 2018.
- [25] P. Latteur, S. Goessens, J.-S. Breton, J. Leplat, Z. Ma, and C. Mueller, "Drone-based additive manufacturing of architectural structures," in *Proceedings of IASS Annual Symposia*, vol. 2015, no. 2. International Association for Shell and Spatial Structures (IASS), 2015, pp. 1–12.
- [26] N. Melenbrink, J. Werfel, and A. Menges, "On-site autonomous construction robots: Towards unsupervised building," *Automation in construction*, vol. 119, p. 103312, 2020.
- [27] E. Gdoutos, A. Truong, A. Pedivellano, F. Royer, and S. Pellegrino, "Ultralight deployable space structure prototype," in *AIAA SciTech 2020 Forum*, 2020, p. 0692.
- [28] G. Kiper and E. Soylemez, "Deployable space structures," in *2009 4th International conference on recent advances in space technologies*. IEEE, 2009, pp. 131–138.
- [29] A. Hanaor and R. Levy, "Evaluation of deployable structures for space enclosures," *International Journal of Space Structures*, vol. 16, no. 4, pp. 211–229, 2001.